Ultrasound contrast agent imaging: Real-time imaging of the superharmonics

D. Peruzzini, J. Viti, P. Tortoli, M. D. Verweij, N. de Jong, and H. J. Vos

Citation: AIP Conference Proceedings **1685**, 040011 (2015); doi: 10.1063/1.4934406
View online: http://dx.doi.org/10.1063/1.4934406
View Table of Contents: http://scitation.aip.org/content/aip/proceeding/aipcp/1685?ver=pdfcov
Published by the AIP Publishing

Ultrasound Contrast Agent Imaging: Real-time Imaging of the Superharmonics

D. Peruzzini[1,2], J. Viti[1,2], P. Tortoli[1], M.D. Verweij[3], N. de Jong [2,3] and H.J. Vos[2,3,a)]

[1] *MSD lab, Department of Information Engineering, Univ of Florence, Via S.Marta, 3, 50139 Firenze, Italy*
[2]*Erasmus MC, 's-Gravendijkwal 230, Faculty Building, Ee 2302, 3015 CE Rotterdam, Netherlands*
[3] *Acoustical Wavefield Imaging, ImPhys, Delft Univ Technology, van der Waalsweg 8, 2628 CH Delft, Netherlands*

[a)] Corresponding author: h.vos@erasmusmc.nl

Abstract. Currently, in medical ultrasound contrast agent (UCA) imaging the second harmonic scattering of the microbubbles is regularly used. This scattering is in competition with the signal that is caused by nonlinear wave propagation in tissue. It was reported that UCA imaging based on the third or higher harmonics, i.e. "superharmonic" imaging, shows better contrast. However, the superharmonic scattering has a lower signal level compared to e.g. second harmonic signals. This study investigates the contrast-to-tissue ratio (CTR) and signal to noise ratio (SNR) of superharmonic UCA scattering in a tissue/vessel mimicking phantom using a real-time clinical scanner. Numerical simulations were performed to estimate the level of harmonics generated by the microbubbles. Data were acquired with a custom built dual-frequency cardiac phased array probe. Fundamental real-time images were produced while beam formed radiofrequency (RF) data was stored for further offline processing. The phantom consisted of a cavity filled with UCA surrounded by tissue mimicking material. The acoustic pressure in the cavity of the phantom was 110 kPa (MI = 0.11) ensuring non-destructivity of UCA. After processing of the acquired data from the phantom, the UCA-filled cavity could be clearly observed in the images, while tissue signals were suppressed at or below the noise floor. The measured CTR values were 36 dB, >38 dB, and >32 dB, for the second, third, and fourth harmonic respectively, which were in agreement with those reported earlier for preliminary contrast superharmonic imaging. The single frame SNR values (in which 'signal' denotes the signal level from the UCA area) were 23 dB, 18 dB, and 11 dB, respectively. This indicates that noise, and not the tissue signal, is the limiting factor for the UCA detection when using the superharmonics in nondestructive mode.

INTRODUCTION

Ultrasound is one of the most used imaging technologies in medicine. It is portable, free of radiation and relatively inexpensive, especially if compared with imaging techniques like magnetic resonance and computed tomography. Ultrasound is used in a diverse range of medical fields. Clinical echocardiography (ultrasonic imaging of the heart) has become routine in the diagnosis and management of heart diseases. Moreover the introduction of ultrasound contrast agent (UCA), consisting of microscopic bubbles of gas enclosed in a thin shell, has widely improved the visualization of vasculature, left-right ventricular shunts, tissue perfusion, and delineation of the cavity of the heart, as needed for wall motion analysis.

Originally, ultrasound systems were tuned to receive only fundamental-frequency echoes. Much improvement in the image quality was gained by exploiting the nonlinear responses, i.e. the harmonic frequencies caused by UCA. A popular technique known as power modulation [1] is based on the pressure-dependent amplitude response of microbubbles. Another technique is contrast harmonic imaging (HI), based on the selective imaging of the second harmonic frequency. Advantages of HI are the improved axial and lateral resolution, and a better suppression of image artifacts [2]. Moreover, to reduce the spectral overlap between the fundamental and the second harmonic nonlinear echo, pulse inversion was introduced and shown capable of solving the compromise between the axial resolution and the transmitted bandwidth [3]. Both pulse inversion and power modulation reduce the imaging frame rate by at least a factor two. Moreover, nonlinear ultrasound propagation occurs in tissue that also generates harmonic components, which severely reduce the contrast to tissue levels [4] in second harmonic mode.

Recent Developments in Nonlinear Acoustics
AIP Conf. Proc. 1685, 040011-1–040011-4; doi: 10.1063/1.4934406

FIGURE 1. Photograph of the setup with a block of tissue mimicking material with cavities, and the probe imaging the region.

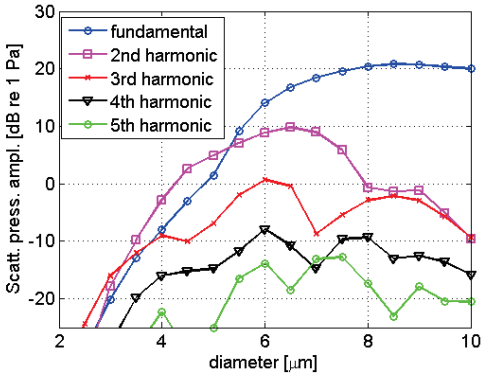

FIGURE 2. Simulated harmonic levels as a function of bubble diameter.

Next to the second harmonic imaging, a modality called superharmonic imaging was proposed to use also the third, fourth, and fifth harmonic bands [5], combining them in an attempt to increase the received energy. This technique has recently gained renewed interest in the form of acoustic angiography [6]. The higher harmonics, even more than the second one, feature narrower -6 dB beam widths (increasing lateral resolution), a shorter time pulse (increasing axial resolution), increased reduction of side lobes, and higher contrast to tissue ratio. The resulting images, therefore, are supposed to show more details than those produced by the second harmonic. This was preliminary shown by Bouakaz et al. (2004), who demonstrated that the contrast between UCA and tissue increases as a function of the order of the harmonic frequency.

In order to use this new imaging modality, subsequent versions of an ultrasonic phased array transducer consisting of two interleaved piezoelectric subarrays with different frequency bands were constructed in the early 2000's [5]. The current version of the transducer [7, 8] had limited application because of absence of suitable research scanners. This paper investigates the use of the probe for superharmonic detection of UCA, associated to a recent programmable ultrasound system by Ultrasonix (Sonix TOUCH). Numerical simulations of the superharmonic behavior of microbubbles in an ultrasound field are also reported.

MATERIALS AND METHODS

Simulation

We used a numerical model defined by Marmottant [9, 10] to describe the radial excursion of a microbubble coated with a thin membrane, in an ultrasound field. The radial dynamics were predicted by solving a nonlinear ordinary differential equation in MATLAB code. The backscattered echo of a single, stationary, isolated, spherical, shelled microbubble surrounded by water was then calculated from the radial dynamics [11]. Material parameters for the bubble coating were described in ref. [10], giving a shear viscosity of $\kappa_s = 6\ 10^{-9}$ Pa.s and a shell elasticity of $\chi = 2.5$ N/m. An initial surface tension of $\sigma_0 = \sigma_w/2 = 0.036$ N/m was assumed. Bubbles with a diameter ranging from 2 µm to 10 µm were simulated. Each bubble was excited by a 110 kPa pulse at 1 MHz containing 2 cycles with a cosine envelope. Attenuation of the backscattered echo of 0.5 dB/cm/MHz was taken into account in the back propagation.

Experiment

We used a dual-frequency phased array probe that was originally developed for cardiac tissue superharmonic imaging. It has interleaved low-frequency transmit elements (N=44, f_c=1 MHz, 50% fractional bandwidth) and high-frequency receive elements (N=44, fc = 3.5MHz, 85% fractional bandwidth). All elements were individually addressed through a custom-programmed commercial ultrasound machine (SonixTOUCH, Ultrasonix with Ultrasonix Texo library) in sector scanning mode. The transmit focus was 6 cm, the echo signals were dynamically focused in receive. Real-time images were produced during the measurements, while beam formed RF data was stored for further offline processing. A tissue mimicking phantom with a UCA-filled cavity of 1 cm diameter was designed to produce realistic tissue and contrast scattering, see Fig. 1. BR14 (Bracco, Geneva) contrast agent was

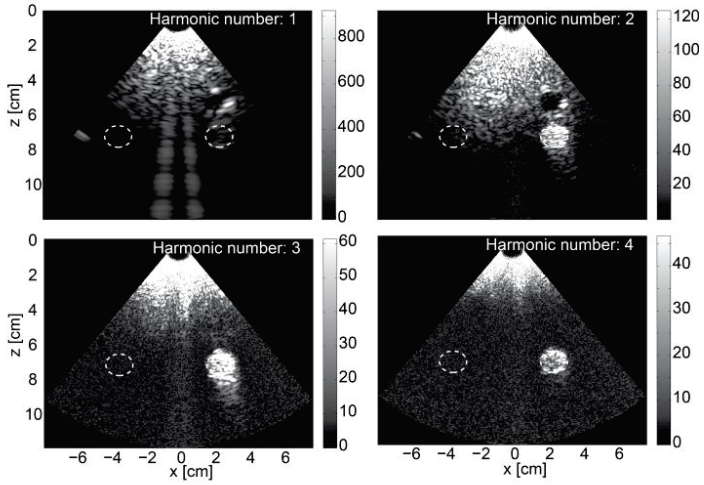

FIGURE 3. Images obtained from the experiment after spectral separation of the subsequent harmonics

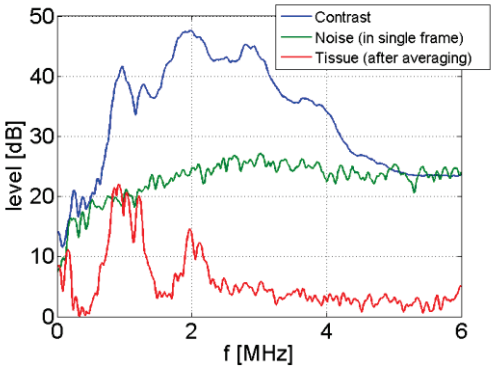

FIGURE 4. Signal spectra in the UCA and tissue regions, and noise levels. The vertical axis is uncalibrated

diluted in a 1:2000 ratio to mimic clinical concentration. The pressure level in the cavity of the phantom was 110 kPa (MI = 0.11, defined by the ratio of peak negative pressure [MPa] and the square root of the frequency [MHz]) ensuring non-destructivity of UCA. Based on single frames captured with the high-frequency elements, the RF data were filtered around the second, third and fourth harmonic, respectively, with high-order 1.1-MHz wide (at -6dB) zero-phase band pass filters. To quantify the signal level, RMS levels from UCA and tissue areas were obtained from the data. The RMS of the noise was obtained with disabled transmission.

RESULTS

Simulation

Figure 2 shows the simulated scatter amplitude as function of the bubble size for the fundamental frequency and its harmonics. For microbubbles larger than 4 µm in diameter, significant signal levels are predicted by the model. Notably, superharmonics are predicted for bubbles larger than 6 µm in diameter, which corresponds to a bubble that is near its resonant regime, in which the oscillation amplitude is significantly large. However, the magnitude varies substantially between the various harmonics. Whereas the second harmonic pressure reaches 3 Pa, the third harmonic reaches 1 Pa at most, and the fourth and fifth harmonic are below 1 Pa. This clearly indicates that the expected superharmonic levels are low, and that only ensembles of microbubbles are expected to be detected. The level of the subsequent harmonics tends to be about 8 dB lower for every harmonic. This 8 dB is caused by about 6 dB lower response of the microbubble itself, and about 2.5 dB lower levels because of the return path attenuation of the echo (0.5 dB/cm/MHz, 5 cm travel path). Since the harmonics caused by the nonlinear propagation in *tissue* are probably even lower [2, 4, 8], it can be expected that the contrast harmonic signals will decrease less than the tissue harmonic signals, which is beneficial for the contrast detection.

Experiment

Figure 3 shows the images of the phantom for fundamental frequency and its harmonics after averaging of 140 consecutive frames. This averaging increased the signal-to-noise ratio in the images, which better revealed the actual tissue levels. If no averaging had been applied, the tissue scattering would be fully shadowed by noise. The water-filled cavity is most clearly visible in the second harmonic image, while the UCA-filled cavity is clearly observed for the fundamental frequency, the second, third and fourth harmonics. The tissue signals were around (for the 2nd harmonic) or below (for 3rd and higher harmonics) the noise floor, indicating that tissue levels were far below the contrast signals.

TABLE 1. Measured SNR and CTR values, in dB

Harmonic number	1	2	3	4
SNR	21	23	18	11
CTR	21	36	>>38	>32

This difference is signal levels is further quantified by calculating the signal spectra (Fig. 4) in the UCA-filled cavity, and in a nearby area in the tissue mimicking material. Since the third and higher harmonics of tissue are below the noise floor, only a value of lower CTR bounds could be obtained for the third and fourth harmonics.

The CTR and SNR values, as obtained from an RMS analysis of the signals leading to Fig. 3, are shown in Table 1. Most clearly, the CTR increases for higher harmonic numbers, which is consistent with the qualitative results in Fig. 3. These values are similar to those so far reported for preliminary contrast superharmonic imaging measurements [5]. The single frame SNR values (in which 'signal' denotes the signal level from the UCA area) are much lower than the CTR, and decrease by about 6 dB with every harmonic number. The trend is consistent with the numerical simulations, although there we found an 8dB decrease for every number. This minor difference may be explained by a possible difference in the real values of the shell parameters as compared to those assumed in the simulation. The lower SNR in the fundamental band (1st harmonic) is caused by a very low sensitivity of the high-frequency elements to this low-frequency component [7].

To study the destruction of the ultrasound contrast agent, we calculated the signal levels over 140 frames, which corresponds to a 18 s time span. The trend of all signals is to decrease by about 3dB, except for the 4th harmonic, which has not decreased significantly. This result shows that the UCA can produce significant superharmonic signals over extended period of time and frames.

CONCLUSION

The experimental values show the improved CTR achieved by superharmonic imaging compared to second harmonic imaging. However, the reduction of SNR values for the increasing harmonic numbers indicate that noise, and not the tissue signal, is the limiting factor for the UCA detection when using the superharmonics in nondestructive mode. This finding is contrary to second harmonic UCA imaging in practice. As implication, increasing the SNR should be the main focus for optimising superharmonic ultrasound contrast imaging, similar to the work recently activated by Harput et al. for tissue superharmonic imaging [12].

REFERENCES

1. A. Novell, J.-M. Escoffre and A. Bouakaz, Curr. Mol. Imag. **2** (1), 77-88 (2013).
2. F. A. Duck, Ultras. Med. Biol. **28** (1), 1-18 (2002).
3. D. H. Simpson, C. T. Chin and P. N. Burns, IEEE Trans. Ultras. Ferr. **46** (2), 372-382 (1999).
4. H. J. Vos, D. E. Goertz and N. de Jong, J. Acoust. Soc. Am. **127** (3), 1208-1217 (2010).
5. A. Bouakaz, F. ten Cate and N. de Jong, Phys. Med. Biol. **49** (16), 3515 (2004).
6. B. D. Lindsey, J. D. Rojas, K. Heath Martin, S. E. Shelton and P. Dayton, IEEE Trans. Ultras. Ferr. **61** (10), 1668-1687 (2014).
7. P. van Neer, PhD Thesis, Erasmus MC Rotterdam (2010).
8. G. M. Matte, P. L. Van Neer, M. G. Danilouchkine, J. Huijssen, M. D. Verweij and N. De Jong, IEEE Trans. Ultras. Ferr. **58** (3), 533-546 (2011).
9. P. Marmottant, S. van der Meer, M. Emmer, M. Versluis, N. De Jong, S. Hilgenfeldt and D. Lohse, J. Acoust. Soc. Am. **118** (6), 3499 - 3505 (2005).
10. M. Overvelde, V. Garbin, J. Sijl, B. Dollet, N. De Jong, D. Lohse and M. Versluis, Ultras. Med. Biol. **36** (12), 2080-2092 (2010).
11. J. Sijl, H. J. Vos, T. Rozendal, N. de Jong, D. Lohse and M. Versluis, J. Acoust. Soc. Am. **130** (5), 3271-3281 (2011).
12. S. Harput, J. McLaughlan, D. M. Cowell and S. Freear, IEEE Trans. Ultras. Ferr. **61** (11), 1802-1814 (2014).